SFDR probability in time-interleaved ADCs with random channel mismatches

Gildas Leger, Eduardo Peralías and Adoración Rueda

Instituto de Microelectrónica de Sevilla (IMSE-CNM), Universidad de Sevilla,
Edificio CICA, c/ Tarfia s/n, 41012-SEVILLA, SPAIN.
email: leger@imse.cnm.es

ABSTRACT:

One of the ways to push the speed limits of Analog to Digital Converters (ADCs) is to time-interleave several channels. However, any mismatch between channels degrades the converter resolution.

The impact of gain and offset mismatches and time skews on the Signal-to-Noise Ratio (SNR) has already been determined. However, no estimation of the Spurious-Free Dynamic Range (SFDR) has been provided to date. This paper gives a probabilistic description of the problem. The Probability Density Function (PDF) of the Spurious-Free-Dynamic Range (SFDR) is explicitly calculated, giving access to important statistical parameters.

RESUMEN:

Se puede conseguir un convertidor analógico-digital de alta velocidad poniendo en paralelo varios convertidores de velocidad media. Sin embargo, cualquier desapareamiento entre los canales reduce la precisión del convertidor final.

El impacto sobre la relación señal-ruido de las diferencias de ganancia y de offset, así como de los errores en los instantes de muestreo de los convertidores ha sido determinado. Sin embargo, el impacto sobre el SFDR no se ha evaluado. Este trabajo da una descripción probabilística del problema. Se calcula explícitamente la función densidad de probabilidad del SFDR, dando así acceso a importantes parámetros estadísticos.

SFDR probability in time-interleaved ADCs with random channel mismatches

Gildas Leger, Eduardo Peralías and Adoración Rueda
Instituto de Microelectrónica de Sevilla (IMSE-CNM), Universidad de Sevilla,
Edificio CICA, c/ Tarfia s/n, 41012-SEVILLA, SPAIN.
email: leger@imse.cnm.es

ABSTRACT

One of the ways to push the speed limits of Analog to Digital Converters (ADCs) is to time-interleave several channels. However, any mismatch between channels degrades the converter resolution.

The impact of gain and offset mismatches and time skews on the Signal-to-Noise Ratio (SNR) has already been determined. However, no estimation of the Spurious-Free Dynamic Range (SFDR) has been provided to date. This paper gives a probabilistic description of the problem. The Probability Density Function (PDF) of the Spurious-Free-Dynamic Range (SFDR) is explicitly calculated, giving access to important statistical parameters.

1. INTRODUCTION

Many applications are requiring faster and faster analog-to-digital converters. In Radio-Frequency design, for example, the trend is to move the analog to digital conversion to front-end or to intermediate frequency, in order to implement digitally the filtering and signal processing. Therefore, very high speeds are expected for the ADCs and literature reports up to 6bits at 1.3GHz [1]. However, these ADCs are usually flash or folding architecture, which are also resolution limited. Thus, it is becoming very difficult to go beyond these limits without losing too much precision or without using exotic and thus expansive technologies (HEMT in GaAs, optical or even superconducting ADCs) [2].

A possible way to gain some speed is to use the time-interleaving technique, first presented by Black and Hodges [3]. Figure 1 shows a general sketch of the system. A number M of medium-speed ADCs are operated in parallel but the sampling instants between two consecutive ADCs are shifted by a fraction 1/M of their clock period. By multiplexing the channel output in a circular form, an equivalent high-speed ADC is obtained, that should have the same precision as the channel ADCs but with a speed M times higher. The only full-speed operation is the multiplexing, which is actually a digital operation. Thus, time-interleaving

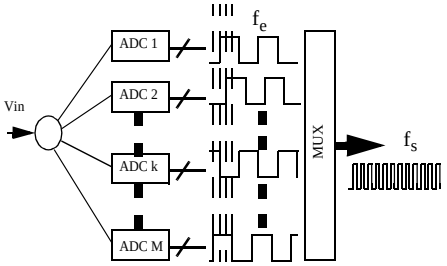

Fig. 1: Scheme of an M-channel time-interleaved ADC.

trades area for speed in an approximately 1:1 ratio and can be used with almost any ADC architecture. Nevertheless, the drawbacks of this technique are two. One of them is that the ADC throughput and bandwidth are increased, but the latency will be the same as for the channel ADCs, which can be critical for some applications. But the most serious issue is that any mismatch between the channels will result in a precision loss.

One important source of mismatch is the presence of time skews in the sampling scheme. If the signal is not uniformly sampled, precision is lost. Apart from time skews, offset and gain mismatches are also specially relevant. Indeed, for a single channel ADC, the exact value of gain or offset is not of much importance, as it will not affect the SNR or SFDR value. But for a time-interleaved architecture much more care should be taken as gain and offset mismatches will generate noise spurs in the signal band.

Estimations of the impact of these three kinds of mismatch on the SNR have already been proposed in other works [5, 6, 7, 8]. And even some solutions to cope with the mismatches have begun to appear in the literature [9, 10, 11]. Nevertheless, this work intends to give a deeper insight to the mismatch issue through a probabilistic treatment, completing the work presented in [12]. A closed expression is developed for the probability density function of the SFDR, as function of the mismatch variance and the number of channels. To our knowledge, this is the first study extracting SFDR information from the channel mismatches.

The paper is organized as follows. Section 2 introduces the basics of the spectral analysis of time

interleaved ADCs. Section 3 derives a closed form for the SFDR probability density function and validates it through simulations. Section 4 draws interesting information from the probabilistic model about the variation of SFDR with the number of channels. And at last Section 6 summarizes the conclusions of this paper.

2. SPECTRAL ANALYSIS

Shannon's theorem implies that an ADC running at f_s cannot convert signal above $f_s/2$, the Nyquist frequency. Indeed, above $f_s/2$, the input signal and its alias at f_s-f_{in} mix and cannot be separated. In a time-interleaved ADC, however, the aliases of all channel ADCs cancel each others when output signals are multiplexed, as can be seen in Fig. 2 for a 2-channels ADC. In this case, each elementary ADC is running at f_e, and after the interleaving the overall sampling frequency passes to be $f_s=2f_e$.

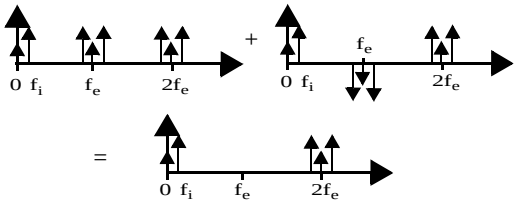

Fig. 2: Alias cancellation in a 2-channels time interleaved ADC

However, if there are mismatches, alias cancellation is not complete and some spurs will remain on the final spectrum. For an M-channel ADC with offset mismatch, spurs will appear at every M^{th} fraction of the sampling frequency (that is, f_s/M, $2f_s/M$,..., $(M-1)f_s/M$). While for gain mismatch and time-skews, spurs will appear like the signal modulated at every M^{th} fraction of the sampling frequency (that is: $f_s/M+f_{in}$, $f_s/M-f_{in}$, $2f_s/M+f_{in}$, $2f_s/M-f_{in}$,...).

In that follows, we will keep the same notation as in [4,5], calling;

M --- the number of interleaved channels

$T=1/f_s$ --- the equivalent sampling period of the ADCs array

t_m --- the real sampling instant of channel m, taking into account the time skews.

$t_m=mT-r_mT$, where r_m is the time skew associated to channel m, expressed as a fraction of the sampling period.

We pretend to study separately the errors due to gain mismatch, offset mismatch and time skews. Hence, the channel ADCs are modelled in the simplest way possible, as a fixed delay followed by a perfectly linear device with variable slope and offset, as seen in Fig. 3.

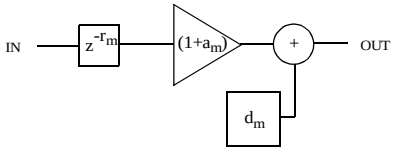

Fig. 3: m^{th} channel discrete-time model

Gain errors are introduced multiplying the signal amplitude by a channel-dependent term, $1+a_m$, while offset errors are considered with an additional term, d_m.

Working in the z-domain and considering the time-interleaved output sequence TI(n) as the sum of the upsampled channel ADC sequences,

$$[\,TI(1)\ TI(2)\ ...\ TI(n)] =$$

$$[ADC_1(1)\ 0\ 0\ 0\ ADC_1(2)\ 0\ 0\ 0\ ADC_1(3)\ 0\ ...\ ]$$

$$+ [0\ ADC_2(1)\ 0\ 0\ 0\ ADC_2(2)\ 0\ 0\ 0\ ADC_2(3)\ ...]$$

$$+ [0\ 0\ ADC_3(1)\ 0\ 0\ 0\ ADC_3(2)\ 0\ 0\ 0\ ADC_3(3)\ ...]$$

$$+ [0\ 0\ 0\ ADC_4(1)\ 0\ 0\ 0\ ADC_4(2)\ 0\ 0\ 0\ ...]$$

the authors in [4] and [5] obtain a general expression of the output spectrum that for the particular case of a sinusoidal input with ω_{in} frequency and A_0 amplitude can be written as,

$$F(\omega) = \frac{1}{MT}\sum_{k=-\infty}^{\infty}\left[\left(\sum_{m=0}^{M-1}\pi A_0(1+a_m)e^{j\omega_{in}r_mT}e^{-jkm\frac{2\pi}{M}}\right)\delta\left(\omega+\omega_{in}-k\frac{2\pi}{MT}\right)\right. \quad (1)$$
$$+\left(\sum_{m=0}^{M-1}\pi A_0(1+a_m)e^{-j\omega_{in}r_mT}e^{-jkm\frac{2\pi}{M}}\right)\delta\left(\omega-\omega_{in}-k\frac{2\pi}{MT}\right)$$
$$\left.+\left(\sum_{m=0}^{M-1}2\pi d_m e^{-jkm\frac{2\pi}{M}}\right)\delta\left(\omega-k\frac{2\pi}{MT}\right)\right]$$

As stated before, we can see that the first two terms of Eq (1) stand for spurs appearing as uncancelled alias of the signal around the M^{th} fractions of the sampling frequency. These two terms are due to both gain mismatch and time-skews. The third term of Eq (1) stands for tones that appear at the M^{th} fractions of the sampling frequency and that are due to offset mismatch.

Obviously, the output spectrum expressed in Eq (1) does not take into account the quantization error. But this is not important because if the mismatch errors are as small as the quantization error, the overall ADC can be considered almost ideal.

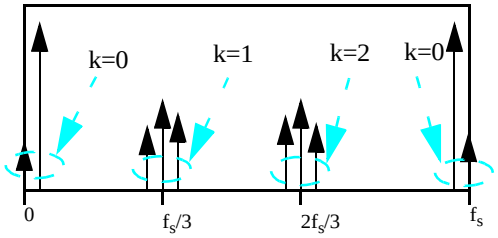

Fig. 4: A spectrum example for a 3-channel interleaved ADC

In order to facilitate the comprehension of the mathematical developments, let us try to establish a clear representation of the spectrum. In Fig. 4, Eq (1) is graphically represented over the band $[0;f_s[$ for the case of a 3-channel ADC.

A more traditional representation of the spectrum would be over the half of this band, from 0 to the Nyquist frequency, $f_s/2$; and in fact it would also handle the whole information, as $F(\omega)=F(2\pi/T-\omega)$. However, it appears to be more difficult to mentally manage the folding of the spurs for different k values over the halves of the signal bands. Over the represented band, the signal is thus given by the terms in $\delta(\omega-\omega_{in})$ and $\delta(\omega+\omega_{in}-2\pi/T)$ (at $k=0$ and at $k=3$ respectively).

If mismatches are kept small, signal power can be written as,

$$P_{signal} = \frac{A_0^2}{2} \qquad (2)$$

3. SFDR Probability Density Function

To introduce the probability treatment, we will assume that all a_m, d_m and r_m in Eq.(1) are random variables distributed with a Normal law[1]. These random variables can be normalized such that,

$$x_m \sim N(0,\sigma_x) \qquad x_m = \sigma_x x^*_m \qquad x^*_m \sim N(0,1) \qquad (3)$$

with x standing for either a, d or r.

In the following development we will consider three initial assumptions:

a) one kind of mismatch will probably dominate over the others, so we will study only one at a time (this would otherwise complicate the treatment unnecessarily)

b) small time skews, which will allow the use of Taylor expansion,

$$e^{-j\omega_{in} r_m T} \approx 1 - j\omega_{in} r_m T = 1 - j2\pi \frac{f_{in}}{f_s} \sigma_r r_m^* \qquad (4)$$

c) the first spur due to the offset mismatch, appearing at $f=0$, is considered as the whole ADC offset.

The procedure to carry out the probabilistic approach is illustrated in Fig. 5.

We will follow the same steps for the 3 types of mismatch. The first step consists in calculating the PDF of the spur power (the spur height), which should depend on the value of k, that defines the spur position in the spectrum. The second step consists in getting the PDF of the highest spur, and the last step finally deduces the SFDR PDF.

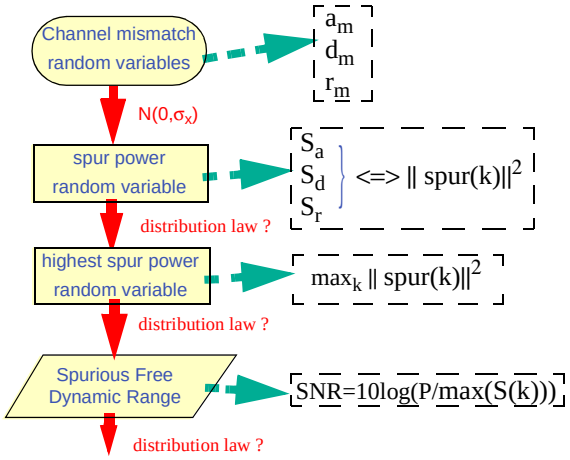

Fig. 5: Procedure leading to the SFDR probability density function.

According to the flow presented in Fig. 5, we have to calculate an expression of the spur power. The power of the offset spur appearing at the k^{th} fraction of the sampling frequency (that is, at kf_s/M) can be expressed as the squared module of the third term in Eq (1).

1. A Normal Law is chosen as it is probably the most conservative assumption if no information on the technology mismatch is available. Moreover, at the ADCs level, the offset and gain mismatches as well as the time-skews can arise from lots of component mismatches. Then, to some extent, we can apply the Central Limit Theorem.

$$P_d^{spur}(k) = \frac{\sigma_d^2}{M^2}\left\|\sum_{m=0}^{M-1} d_m^* e^{-jkm\frac{2\pi}{M}}\right\|^2 = \frac{\sigma_d^2}{M^2} S_M^d(k) \qquad (5)$$

We recall that the case *k=0* is not considered in this study, as the spur in DC is considered as the overall ADC offset.

Here it is important to notice that the spur power should depend on the value of *k*. However, it is easily verified that,

$$S_M^d(k) = \left\|\sum_{m=0}^{M-1} d_m^* e^{-jkm\frac{2\pi}{M}}\right\|^2 = \left\|\sum_{m=0}^{M-1} d_m^* e^{-j(M-k)m\frac{2\pi}{M}}\right\|^2 \qquad (6)$$

This actually means that the spur at $(kf_s)/M$ will have the same height as the spur at $((M-k)f_s)/M$. Therefore, only the spurs corresponding to the integers *k* comprised between 1 and M/2 have to be considered for SFDR calculation.

For the gain mismatch the result is very similar. Moreover, we can notice that the second and the third term in Eq (1) (the spurs at $(kf_s)/M + \omega_{in}$ and $(kf_s)/M - \omega_{in}$ respectively) will also have the same module, and thus only one of them should be considered in the SFDR calculation. For the time-skews, the result presents a little difference as the uncancelled aliases around a sampling frequency fractions will not have the same amplitude. However, if the terms r_m are kept small, this difference will also be very small and thus only one of the two aliases can be taken into consideration for the SFDR calculation. This is equivalent to neglecting the orders higher than 1 in the Taylor development of Eq (4).

Then, the power of the spurs for a gain mismatch can be written as,

$$P_a^{spur}(k) = \frac{A_0^2\sigma_a^2}{4M^2}\left\|\sum_{m=0}^{M-1} a_m^* e^{-jkm\frac{2\pi}{M}}\right\|^2 = \frac{A_0^2\sigma_a^2}{4M^2} S_M^a(k) \qquad (7)$$

And for the time-skews,

$$P_r^{spur}(k) = \frac{A_0^2\sigma_r^2}{4M^2}\times(2\pi)^2\left(\frac{f_{in}}{f_s}\right)^2\left\|\sum_{m=0}^{M-1} r_m^* e^{-jkm\frac{2\pi}{M}}\right\|^2 = \frac{A_0^2\sigma_r^2}{4M^2}\times(2\pi)^2\left(\frac{f_{in}}{f_s}\right)^2 S_M^r(k) \qquad (8)$$

It appears clearly that the probability treatment will be the same for all the three mismatch contributions, as the term S^x_M has the same form in Eq (6), Eq (7) and Eq (8). Therefore, we will thus treat the case of the offset mismatch and then take the results to the gain mismatch and time-skew cases.

We have obtained an equation relating the spur power to the mismatch random variables. So the next step of the flow described in Fig. 5 consists in finding the probability density function of the spur power.

Let us consider the case M=4. The first spur at *k=1* is computed as the sum of the channels offset over the 4th-order roots of unity (see Fig. 6). For *k=3*, it is easily seen that spur power would be the same as for k=1, accordingly to Eq (6). However, for *k=2*, the sum is realized over the square roots of unity, in only one dimension of the phase plane.

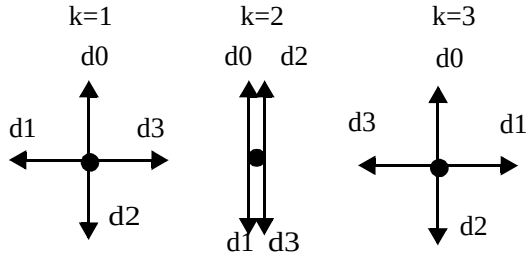

Fig. 6: spur generation in function of k for M=4.

For *k=1* the power would behave as,

$$S_4(1) = (d_0^* - d_2^*)^2 + (d_1^* - d_3^*)^2 \qquad (9)$$

But for *k=2* it would behave as,

$$S_4(2) = (d_0^* + d_2^* - d_1^* - d_3^*)^2 \qquad (10)$$

For other values of M (See Fig. 7 for the case of M=5), the same phenomenon can be observed: if *k* is different from M/2 (which is always the case when M is odd) the spurs would have the same type of PDF, but when *k*=M/2, the PDF would be different. Normally, if M is different from 4, the offset contributions should be projected on the two dimensions of the phase plane. Despite this fact and due to the circular symmetry of the roots, the spurs behave as if there were M/2 contributions on one dimension and M/2 on the other.

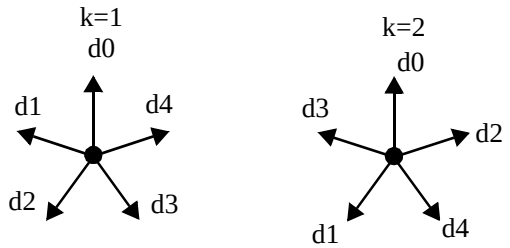

Fig. 7: spur generation asfunction of k for M=5.

Extending Eq (9) and Eq (10), we have, for *k* different from M/2,

$$S_M(k) \Leftrightarrow \left(\sum_{i=1}^{\frac{M}{2}} d_i^* \right)^2 + \left(\sum_{j=\frac{M}{2}+1}^{M} d_j^* \right)^2 \qquad (11)$$

The sum of *n* variables distributed as a Normal law *N(0,1)* is distributed as a Normal law $N(0, n^{1/2})$, and the sum of two squared variables distributed as a Normal law is distributed as a Chi-square law with two degrees of freedom, also known as Rayleigh law [12]. So Eq (11) leads to,

$$S_M\left(k \neq \frac{M}{2}\right) \sim \frac{1}{M} e^{-\frac{x}{M}} = f_o(x) \qquad x > 0 \qquad (12)$$

For *k*=M/2

$$S_M(k) \Leftrightarrow \left(\sum_{i=1}^{M} d_i^* \right)^2 \qquad (13)$$

as all d_i* are distributed as normal laws, Eq (13) leads to,

$$S_M\left(k = \frac{M}{2}\right) \sim \frac{1}{\sqrt{2\pi M x}} e^{-\frac{x}{2M}} = f_e(x) \qquad x > 0 \qquad (14)$$

Another important approximation that we will make is that all spurs are independent. This is obviously not true, but the fact that for different spurs the offset contributions are summed in a different "order" compensates the fact that the contributions are actually the same (See Fig. 7).

Thus, using Eq (6), we can write,

$$SFDR = 10\log\left(\frac{P_{signal}/2}{max(P_{spur})}\right) = 10\log\left(\frac{M^2 A_0^2}{4\sigma_d^2 max_k(S_M(k))}\right) \qquad (15)$$

Here, it is important to notice that the total signal power has been calculated over the whole band and thus it consists of two signal spectral lines, one at f_{in} and another at f_s-f_{in}. Thus the height of one signal spectral line is $P_{signal}/2$.

As stated in [12], the cumulate density function (CDF) of the maximum of a set of independent random variables is the product of their individual cumulate density functions. Moreover, the probability density function is the derivative of the cumulate density function. As we consider that all spurs in the range,

$$k \in \left[1; \frac{M}{2}\right] \quad k \in \aleph \qquad (16)$$

are independent, the probability density function of the maximum comes to be:

a) if M is odd, all (M-1)/2 spurs have the distribution of Eq (12),

$$max_k(S_M(k)) \sim f_o^{max} = \frac{M-1}{2} F_o^{\frac{M-3}{2}} f_o \qquad (17)$$

b) if M is even, (M/2-1) spurs behave as Eq (12) and the spur at *k*=M/2 behaves as Eq (14)

$$max_k(S_M(k)) \sim f_e^{max} = F_o^{\left(\frac{M}{2}-2\right)} \left[\left(\frac{M}{2}-1\right) F_e f_o + f_e F_o\right] \qquad (18)$$

The expressions for f_o and f_e are given in Eq (12) and Eq (14). F_o and F_e are their respective integrals (the CDFs), considering that we must have $F(\infty) = 1$,

$$F_o(x) = \left(1 - \exp\left(\frac{-x}{M}\right)\right) \qquad x > 0 \qquad (19)$$

$$F_e(x) = erf\left(\sqrt{\frac{x}{2M}}\right) \qquad x > 0 \qquad (20)$$

The next step to obtain the SFDR probability density function is to realize the variable change in Eq (15). As the relation between SFDR and $max_k(S_M(k))$ is a bijection, we have,

$$P_{\Phi}(\Phi(x) = t) = P_x(\Phi^{-1}(t)) \left| \frac{d}{dt}(\Phi^{-1}(t)) \right| \qquad (21)$$

where, for the offset mismatch,

$$\Phi(x) = 10\log\left(\frac{M^2 A_0^2}{4\sigma_d^2 x}\right) \quad \text{and}$$

$$\Phi^{-1}(t) = \frac{M^2 A_0^2}{4\sigma_d^2} \exp\left(-\frac{t}{10}\ln(10)\right) \qquad (22)$$

for the gain mismatch,

$$\Phi(x) = 10\log\left(\frac{M^2}{\sigma_a^2 x}\right) \quad \text{and}$$

$$\Phi^{-1}(t) = \frac{M^2}{\sigma_a^2} \exp\left(-\frac{t}{10}\ln(10)\right) \qquad (23)$$

and for the time-skews,

$$\Phi(x) = 10\log\left(\frac{M^2}{\left(2\pi\sigma_r\frac{f_{in}}{f_s}\right)^2 x}\right) \quad \text{and}$$

$$\Phi^{-1}(t) = \frac{M^2}{\left(2\pi\sigma_r\frac{f_{in}}{f_s}\right)^2}\exp\left(-\frac{t}{10}\ln(10)\right) \qquad (24)$$

And the SFDR probability density function comes to be:

a) for M odd,

$$P(SFDR = t) = \left(\frac{M-1}{2}\right)\frac{\ln(10)}{10}\Phi^{-1}(t)\exp\left(\frac{-\Phi^{-1}(t)}{M}\right) \qquad (25)$$
$$\times\left(1-\exp\left(\frac{-\Phi^{-1}(t)}{M}\right)\right)^{\left(\frac{M-3}{2}\right)}$$

b) for M even,

$$P(SFDR = t) = \frac{\ln(10)}{10}\Phi^{-1}(t)\left(1-\exp\left(\frac{-\Phi^{-1}(t)}{M}\right)\right)^{\frac{M}{2}-2} \qquad (26)$$
$$\left[\left(\frac{1}{2}-\frac{1}{M}\right)\exp\left(\frac{-\Phi^{-1}(t)}{M}\right)erf\left(\sqrt{\frac{\Phi^{-1}(t)}{2M}}\right)\right.$$
$$\left.+\frac{1}{\sqrt{2\pi M\Phi^{-1}(t)}}\left(1-\exp\left(\frac{-\Phi^{-1}(t)}{M}\right)\right)\exp\left(\frac{-\Phi^{-1}(t)}{2M}\right)\right]$$

Where the term $\Phi^{-1}(t)$ corresponds to Eq (22) in the case of offset mismatches, to Eq (23) in the case of gain mismatches and to Eq (24) in the case of time skews.

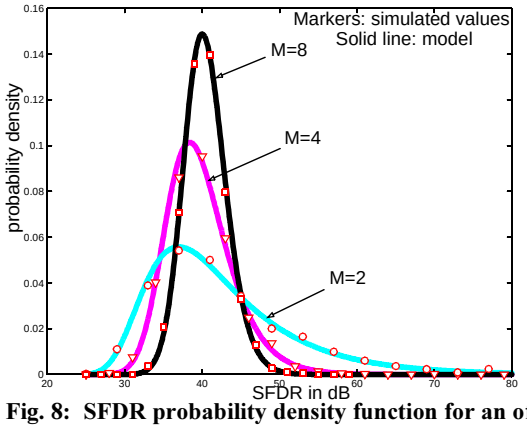

Fig. 8: SFDR probability density function for an offset mismatch of σ_d=0.01, A_0 =1 and M even

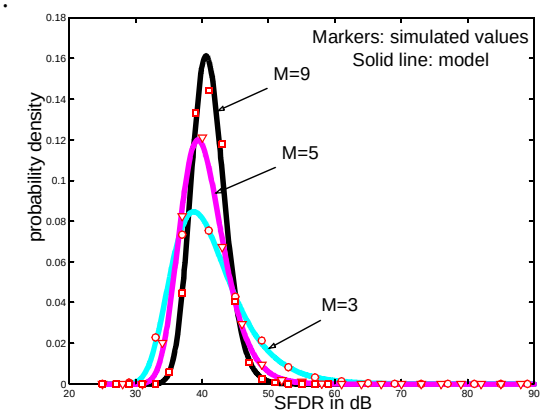

Fig. 9: SFDR probability density function for an offset mismatch of σ_d=0.01, A_0 =1 and M odd

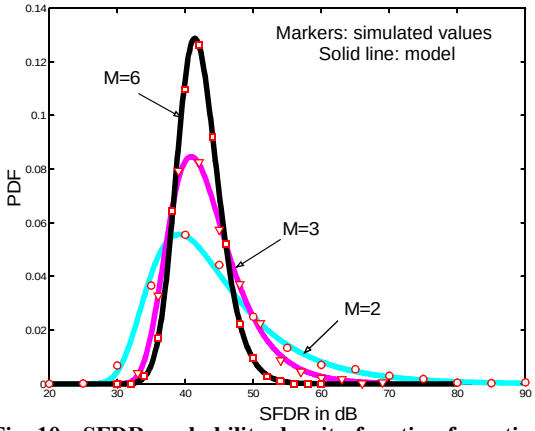

Fig. 10: SFDR probability density function for a time-skew of σ_r=0.005.

In order to verify the correctness of these probability density functions, the calculated results were compared to 2000 Monte Carlo simulations of a virtual 14-bits M-time interleaved ADC. For each run, M random offsets were sampled from a N(0,σ_d) law and applied to the channel ADCs. The FFT of the distorted sine-wave output was then obtained and the SFDR was evaluated.

Fig. 8 and Fig. 9 shows that SFDR does spread over the distribution predicted by the mathematical model, for either even or odd values of M.

Figure 10 presents the same kind of simulation, but for time skews with σ_r=*0.005* and $f_{in}=f_s/2$. Here again, the matching between the model and the simulation is very good. In Fig. 11, an ADC with 4 channels has been simulated for different values of time-skews. The results are also in good agreement with the prediction. Moreover we can notice that, as for the SNR, the dispersion does not depend on the amplitude of the time-skews.

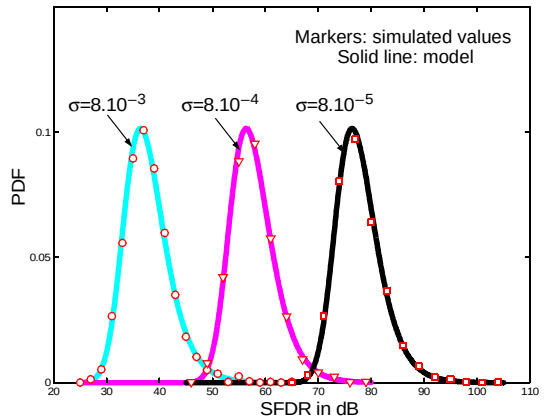

Fig. 11: SFDR probability density function for M=4, with different time-skews.

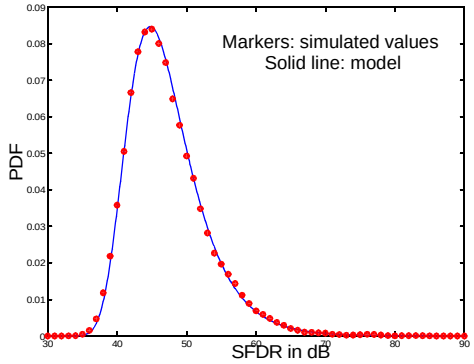

Fig. 12: SFDR probability density function for a gain mismatch of σ_a=0.01 and M=3

For gain mismatches the results are very similar to the results for time-skews and offset mismatch. Thus, Fig. 12 only presents one curve, showing a very good matching between the simulation and the model for a 3-channel ADC with a 1% gain mismatch. However, for this curve, 10000 Monte Carlo runs were realized instead of 2000, in order to get more comparison points.

4. SFDR INFORMATION

Figure 13 shows the evolution of the expected SFDR together with its standard deviation, which have been calculated from the SFDR PDF.

This figure leads us to comment three interesting issues. The first one is that the SFDR increases with the number of channels. This trend could be expected, as the mean total noise had been seen to remain almost constant [11] with the number of channels. Indeed, when the number of channel is increased, more spurs appear in the signal band, and the noise spreads over all

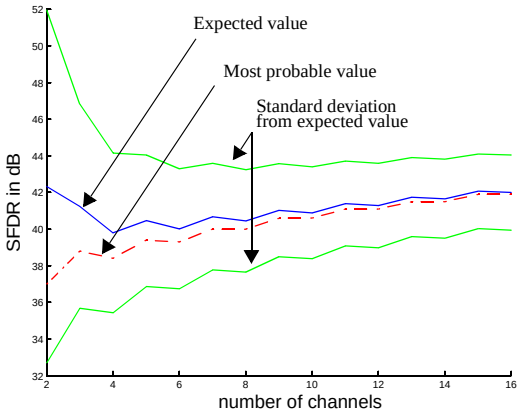

Fig. 13: SFDR Prediction for an offset mismatch of σ_d=0.01 and A_0 =1.

the spurs. As a result, the mean height of each spur decreases and the SFDR increases. However, this trend is not as significant as it could be expected (only 3dB are gained from 2 to 8 channels instead of 6dB). This can be explained by the fact that the SFDR does not rely on the mean spur but on the highest spur. The overall spur height decreases but this is compensated by the fact that there are more spurs, and thus more possibility to get a high spur.

The second interesting issue is that even channel numbers give worse SFDR results than odd channel numbers. This is due to the fact that the spurs which correspond to k=M/2 (for M even), have a more dispersed height than the others, making them more likely to be the maximum spur, which determines the SFDR.

And the last issue that is worth commenting is the SFDR dispersion.Usually most designs are likely to implement a small number of channels in order to limit the chip area. But as can be seen in Fig. 13, for small values of M, the SFDR dispersion is quite large. More concretely, for M=2 the standard deviation is as large as 10 dB. Therefore, this information should be taken into account when fixing the design goals, for example using the PDF to evaluate the convenient confidence intervals.

5. CONCLUSIONS

Time-interleaving is an appealing technique to improve the analog to digital conversion speed for any ADC architecture. However, this strategy will damage the ADC resolution unless the channel mismatches are kept small.

In this paper, the impact of the gain and offset mismatches, as well as of the time-skews on the SFDR

of the resulting ADC has been studied from a probabilistic point of view. The obtained expressions for the Probability Density Function provide designers with important information which should help to solve design trade-off, to tailor safer margins or to fix clear goals for developing mismatch calibration strategies.

Acknowledgement: This work has been partially supported by the European Project SPRING-IST-1999-12342.

6. REFERENCES

[1] M. Choi, A.A. Abidi: "A 6-b 1.3-Gsample/s A/D converter in 0.35- mu m CMOS", *IEEE J. of Solid-State Circuits,* vol.36, no.12; pp.1847-58; Dec. 2001

[2] R.H. Walden: "Analog-to-digital converter survey and analysis", *IEEE J. on Selected Areas in Communications,* vol. 17, no.4; April 1999.

[3] W.C. Black-Jr; D.A. Hodges:"Time interleaved converter arrays", IEEE J. of Solid-State Circuits. vol.SC-15, no.6; pp.1022-9; Dec. 1980

[4] Y.C. Jenq: "Digital Spectra of Nonuniformly Sampled Signals: Fundamentals and High-Speed Waveform Digitizers", *IEEE Trans. on Instrumentation and Measurements,* vol. 37, no.2, pp. 245-251, June 1997.

[5] M. Gustavsson, J.J: Wilkner, N.N. Tan: *"CMOS Data Converters for Communications",* Kluwer Academic Publishers, 2000

[6] N. Kurosawa; H. Kobayashi; K. Maruyama; H. Sugawara; K. Kobayashi: "Explicit analysis of channel mismatch effects in time-interleaved ADC systems", *IEEE Trans. on Circuits and Systems I: Fundamental Theory and Applications,* vol.48, no.3; pp.261-71; March 2001

[7] A. Petraglia-A, S.K. Mitra: "Analysis of mismatch effects among A/D converters in a time-interleaved waveform digitizer" *IEEE Trans. on Instrumentation and Measurement,* vol.40, no.5; pp.831-835; October 1991

[8] J.E. Eklund, F. Gustafsson: "Digital offset compensation of time-interleaved ADC using random chopper sampling", *Proc. of ISCAS 2000; vol. 3, pp. 447-450; 2000*

[9] Daihong-Fu, K.C. Dyer, S.H. Lewis, P.J. Hurst: "A digital background calibration technique for time-interleaved analog-to-digital converters" *IEEE Journal-of-Solid-State-Circuits,* vol.33, no. 12, pp.1904-1911; Dec.1998

[10] Y.C. Jenq: "Perfect Reconstruction of Digital Spectrum from Nonuniformly Sampled Signals" *IEEE Trans. on Instrumentation and Measurements,* vol. 46, n×3, pp. 649-652; June 1997.

[11] G. Leger, E. Peralías, A. Rueda: "SNR probability in time-interleaved ADCs with random channel mismatches" *Proc. of ISCAS 2002*; vol 2, pp. 380-383, 2002

[12] A. Papoulis: *"Probability, Random Variables, and Stochastic Processes",* McGRAW-HILL International Editions, third edition, 1991.